

# ENVIRONMENTAL RESEARCH BRIEF

## Long-term Performance of Permeable Reactive Barriers Using Zero-valent Iron: An Evaluation at Two Sites

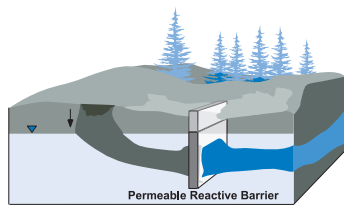
Richard T. Wilkin\*, Robert W. Puls\*, and Guy W. Sewell\*

### Background

The permeable reactive barrier (PRB) technology is an in-situ approach for remediating groundwater contamination that combines subsurface fluid flow management with a passive chemical treatment zone. Removal of contaminants from a groundwater plume is achieved by altering chemical conditions in the plume as it moves through the reactive barrier. Because the reactive barrier approach is a passive treatment, a large plume can be treated in a cost-effective manner relative to traditional pump-and-treat systems. There have now been more than forty implementations of the technology in the past six years, which have proven that passive reactive barriers can be cost-effective and efficient approaches to remediate a variety of compounds of environmental concern. However, in all of the installations to date comparatively few data have been collected and reported on the long-term performance of these in-situ systems, especially with respect to the buildup of surface precipitates or biofouling (O'Hannesin and Gillham, 1998; McMahon et al., 1999; Puls et al., 1999; Vogan, 1999; Phillips et al., 2000; Liang et al., 2000).

A detailed analysis of the rate of surface precipitate buildup in these types of passive, in-situ systems is critical to understanding how long these systems will remain effective and what methods may be employed to extend their lifetime or to improve their performance. Different types of minerals and surface coatings have been observed to form under different geochemical conditions that are dictated by aquifer chemistry and the composition of the permeable reaction zone (Powell et al., 1995; Mackenzie et al., 1999; Liang et al., 2000). Microbiological impacts are also important to understand in order to better predict how long these systems will remain effective in the subsurface (Scherer et al., 2000). The presence of a large reservoir of iron coupled with plentiful substrate availability supports the metabolic activity of iron-reducing, sulfate-reducing, and/or methanogenic bacteria. This enhanced microbial activity may beneficially influence zero-valent iron reductive dehalogenation reactions through favorable impacts to the iron surface or through direct microbial transformations of the target compounds. However, this enhancement may come at the expense of faster corrosion leading to faster precipitate buildup and potential biofouling of the permeable treatment zone.

This research brief presents findings over the past four years at two sites where detailed investigations by the U.S. Environmental Protection Agency (U.S. EPA) have focused on the long-term performance of PRBs under a Tri-Agency Permeable Reactive Barrier Initiative (TRI). This initiative involves the U.S. EPA, the Department of Defense, and the Department of Energy. The objectives of the TRI are to leverage the technical and financial resources of the three agencies in order to examine the field performance of multiple PRBs across the United States. A survey of existing PRBs indicated that the two main challenges facing the technology were (1) uncertainties associated with the longevity (geochemistry) of a PRB and (2) ensuring/verifying hydraulic performance. Therefore, this initiative and our research have focused primarily on these challenges.



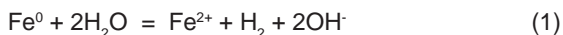
\* U.S. EPA, Office of Research and Development, National Risk Management Research Laboratory, Subsurface Protection and Remediation Division, Ada, OK.

## Introduction

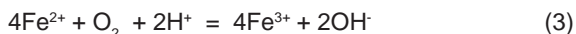
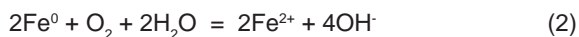
Research described in this research brief explores the geochemical and microbiological processes occurring within zero-valent iron treatment zones in permeable reactive barriers that may contribute to decreases in iron reactivity and decreases in reaction zone permeability that, in turn, may eventually lead to system plugging and failure. Using advanced surface analytical techniques together with detailed coring and water sampling programs at two geographically, hydrogeologically, and geochemically distinct iron barrier installation sites, specific objectives of this research project were to:

- 1) Characterize the type and nature of surface precipitates forming over time at the upgradient aquifer/iron interface, within the iron zone, and at the downgradient/iron interface.
- 2) Develop conceptual models that predict the type and rate of precipitate formation based on iron characteristics and water chemistry.
- 3) Identify type and extent of microbiological activity upgradient, within and downgradient in at least one of the chosen sites to evaluate microbiological response or effects from emplaced iron into an aquifer system.
- 4) Develop practical and cost-effective protocols for long-term performance assessments at permeable reactive barrier installations.

In planning groundwater remediation systems using permeable treatment walls, granular iron metal is the treatment material most often proposed and used. The choice of zero-valent iron stems from the reducing conditions created by reactions between groundwater and iron metal. The "ideal" iron wall would support fast and complete contaminant transformation, and have a hydraulic conductivity that could be maintained over time. However, physical and chemical properties of the iron treatment zone will change with time as a result of the "aging" of the iron. The lifetime of an iron wall will essentially be determined by how fast and by what types of minerals precipitate within the reaction zone. The corrosion of zero-valent iron in aqueous environments has been widely studied (e.g., Reardon, 1995). In water, zero-valent iron is oxidized by many substances to ferrous ion, leading to dissolution and volume loss of the metal. Under anaerobic conditions, reduction of water occurs:



Under aerobic conditions, dissolved oxygen acts as the oxidant and can lead to the production of ferrous and ferric iron:



Both aerobic and anaerobic iron corrosion reactions lead to an increase in pH. Aerobic corrosion is a more rapid process, as evidenced by the rapid loss of dissolved oxygen in iron/water systems. As the corrosion process proceeds, iron hydroxides form, which increases the thickness of an iron oxide passivation layer already present at the iron metal surface. Under anaerobic conditions, hydrogen gas that is formed as a product of iron corrosion may also temporarily passivate the iron surface. Many species abundant in groundwater can affect the iron corrosion process. For example, chloride, carbonate, and sulfate can all accelerate the corrosion of iron by increasing the dissolution rate of the protective oxide layer.

In groundwater, any of the common anions present may influence the effectiveness of zero-valent iron barriers for contaminant remediation. Carbonate is of particular interest. At the high pH condition caused by the corrosion of iron, bicarbonate reacts with  $\text{OH}^-$  and  $\text{Ca}^{2+}$  ions to form insoluble  $\text{CaCO}_3$  that will precipitate as calcite or the polymorph, aragonite. In addition, the bicarbonate anion can precipitate with ferrous ion to form ferrous carbonate (siderite):



Under aerobic conditions, ferric oxides and oxyhydroxides precipitate. Under anaerobic conditions and at high pH, ferrous hydroxide or green-rust minerals are expected to form. Other species in groundwater can also precipitate at the high pH, reducing conditions created in the iron-water system, such as iron sulfides. The formation of these various precipitates has been observed in numerous studies investigating the use of zero-valent iron for remediating contaminated groundwater (e.g., Powell et al., 1995; Mackenzie et al., 1999; Phillips et al., 2000). These mineral precipitates may limit access to the iron surface and thereby decrease reactivity and will decrease porosity and therefore impact flow through the reactive media, resulting in decreased residence time and incomplete treatment of contaminants.

Many studies have investigated the interactions of bacteria with metallic iron under both aerobic and anaerobic conditions. The oxidation or corrosion of zero-valent iron may be stimulated or inhibited by microorganisms (Morales et al., 1993; Hernandez et al., 1994). However from an ecological perspective, metallic iron in subsurface environments represents a significant energy reservoir—an energy supply that microorganisms will utilize if possible. Due to the limited solubility of oxygen in groundwater and the rapid reduction of molecular oxygen by  $\text{Fe}(0)$  and  $\text{Fe}(\text{II})$ , permeable reactive barriers usually exist as anaerobic environments. Under anaerobic conditions molecular oxygen-driven chemical corrosion rates may be reduced, but biologically mediated anaerobic corrosion may occur at rates exceeding those seen under oxygenated conditions (Lee et al., 1995). In the absence of oxygen, protons may serve as electron acceptors and allow for the formation of oxidized iron species such as  $\text{Fe}(\text{II})$ . Under static and aseptic conditions this process is usually limited by the formation of a stable hydrogen film produced from the reduction of protons on the metal surface. However, processes that consume hydrogen gas and thereby interfere with the formation of this hydrogen film, such as mixing with water that is undersaturated with respect to hydrogen or the activity of hydrogen-consuming bacteria, will enhance anaerobic iron corrosion. Both of these processes are likely to be important in PRBs installed in subsurface environments.

The enhancement of the anaerobic corrosion process and the formation of dissolved  $\text{Fe}(\text{II})$  is not necessarily detrimental to PRB performance. If the target contaminant is reduced by  $\text{Fe}(\text{II})$  as well as  $\text{Fe}(0)$ , such as  $\text{Cr}(\text{VI})$ , a dispersion of aqueous  $\text{Fe}(\text{II})$  could represent an increase in the size of the reaction/treatment zone as compared to the surface contact area of  $\text{Fe}(0)$  alone. However, the utilization of dissolved hydrogen may result in bacterial growth and biofilm formation. The development of this biofilm in a PRB may be detrimental to performance through several mechanisms. A microbial biofilm containing iron-reducing and sulfate-reducing bacteria as terminal oxidizers is a complex structure containing both organic and inorganic materials (Cord-Ruwish, 2000). These biofilms are typically only about 5% dry weight, suggesting a disproportionate effect on hydraulics per

unit of bacterial growth. Changes in PRB hydraulic conductivity, the masking of active sites, the removal of active chemical species, and the competition for reducing equivalents would all seem to be processes that could negatively affect PRB performance. Conversely some microbial processes could enhance PRB performance. In some instances bacteria may be more effective at contaminant transformation or may degrade compounds unaffected by PRBs. It is therefore evident that a clear understanding is needed of microbial/PRB interactions for the design and efficient operation of PRBs and because inhibition of biofilm formation under the conditions associated with subsurface PRBs appears to be technically and economically impractical.

### Site Descriptions

Two field sites were evaluated in the U.S. EPA portion of the TRI: the U.S. Coast Guard Support Center (USCG-SC) site near Elizabeth City, North Carolina, and the Denver Federal Center (DFC) in Lakewood, Colorado.

#### U.S. Coast Guard Support Center

The USCG-SC is located about 100 km south of Norfolk, Virginia and 60 km inland from the Outer Banks region of North Carolina. The base is situated on the southern bank of the Pasquotank River, about 5 km southeast of Elizabeth City, North Carolina. A hard-chrome plating shop was in operation for more than 30 years

in Hangar 79, which is only 60 m south of the river (Figure 1). Following its closure in 1984, soils beneath the shop were found to contain chromium concentrations up to 14,500 mg/kg. Subsequent site investigations by U.S. EPA personnel identified a chromate plume extending from beneath the shop to the river. The plume has high (>10 mg/L) concentrations of chromate, elevated sulfate (to 150 mg/L), and minor amounts of chlorinated solvent compounds (trichloroethylene, cis-dichloroethylene, vinyl chloride). The plating shop soils and related groundwater contamination are referred to as solid waste management unit (SWMU) number 9 by the state of North Carolina and the USCG. Sampling results from a monitoring network consisting of more than 40 monitoring wells and about 100 Hydropunch™ and Geoprobe™ monitoring points indicate that the Cr(VI) plume is about 35 m wide, extends to 6.5 m below ground surface and extends laterally about 60 m from the hangar to the Pasquotank River. Multilevel samplers installed near the barrier wall location indicate that the bulk of the contamination resides from 4.5 to 6.5 m below ground surface.

The site geology has been described in detail elsewhere (Puls et al., 1999), but essentially consists of typical Atlantic coastal plain sediments, characterized by complex and variable sequences of surficial sands, silts and clays. In general the upper 2 m of the aquifer are sandy to silty clays that pinch out towards the north, or near the Pasquotank River, where sandy fill predominates. Fine sands, with varying amounts of silt and clay, and silty-clay lenses form the rest of the shallow aquifer.

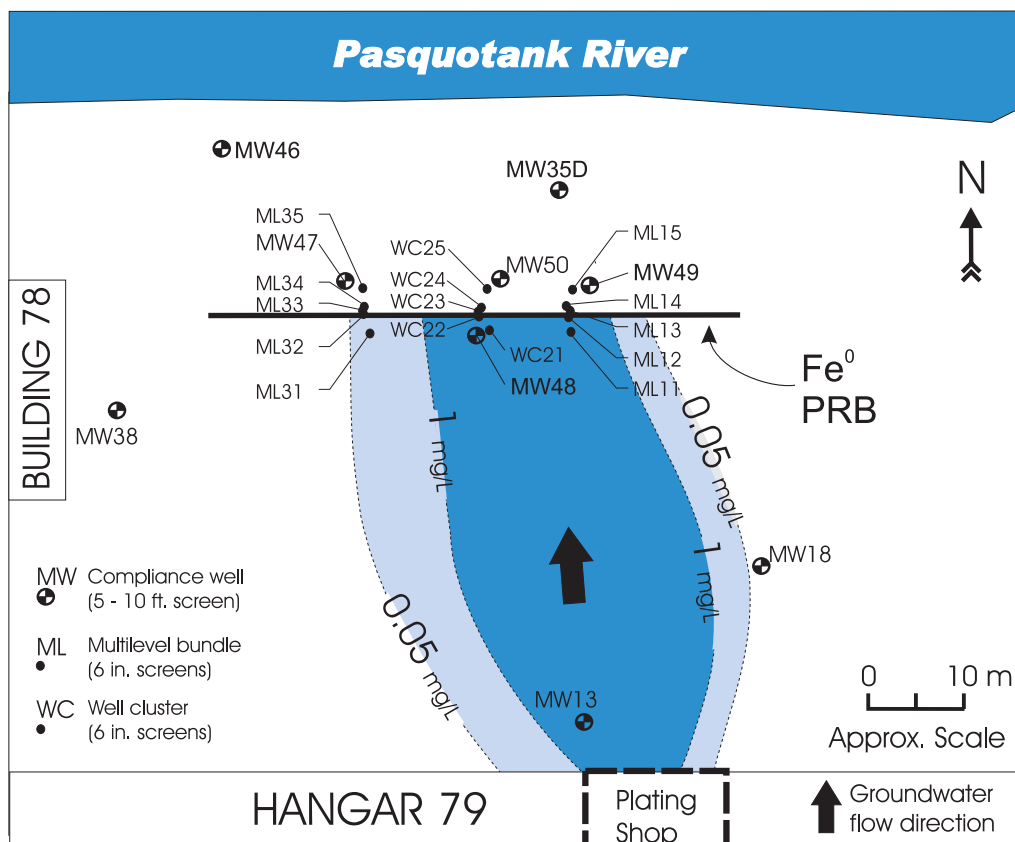


**Figure 1.** Plan view map showing compliance well, bundle and well cluster locations relative to granular iron barrier and Cr plume (June 1994 data).

Groundwater flow velocity is extremely variable with depth, with a highly conductive layer at roughly 4.5 to 6.5 m below ground surface. This layer coincides with the highest aqueous concentrations of chromate. The groundwater table ranges from 1.5 to 2.0 m below ground surface and the average horizontal hydraulic gradient varies from 0.0011 to 0.0033. Slug tests conducted on monitoring wells with 1.5 m screened intervals between 3 and 6 m below ground surface indicate hydraulic conductivity values of between 0.3 to 8.6 m/d. A multiple borehole tracer test in wells screened between 3.9 to 5.9 m below ground surface was conducted by Puls et al. (1999). Groundwater velocities of 0.13 and 0.18 m/day were measured in this test. Assuming an average hydraulic gradient of 0.0023 and porosity of 0.38, these velocities correspond to an average hydraulic conductivity of about 26 m/day. The groundwater is contaminated with chromate and volatile organic compounds including trichloroethylene (TCE), cis-dichloroethylene (cis-DCE), and vinyl chloride (VC).

In June of 1996, a 46 m long, 7.3 m deep, and 0.6 m wide permeable reactive barrier (continuous wall configuration) of zero-valent iron was installed approximately 30 m from the Pasquotank River (Figure 1; Blowes et al., 1999a,b). The reactive wall was designed to remediate hexavalent chromium-contaminated groundwater, in addition to treating portions of a larger overlapping plume of TCE. A detailed monitoring network of over 130 subsurface sampling points was installed in November of 1996 to provide detailed information on spatial and temporal changes in porewater geochemistry.

### **Denver Federal Center**

The Denver Federal Center (DFC) is located about 10 km west of downtown Denver, Colorado. Aquifer materials at the site are made up of alluvial sediments that overlie the Denver Formation. The Denver Formation is Paleocene to Late Cretaceous in age and consists of brown, yellowish-brown, gray, and blue-gray intercalated sandstone, claystone, siltstone, shale and conglomerate containing olive-brown andesitic sandstone beds. It lies about 2 to 14 m below ground surface at the DFC and can attain a thickness of up to 260 m. The Denver Formation has been divided into two zones, the upper weathered zone and a lower unweathered zone. These two zones are lithologically similar but differ in color and permeability, with the upper weathered zone having greater fracture permeability. The upper weathered zone is up to 7 m thick and exhibits a grayish brown color with yellowish orange staining while the lower unweathered zone has a diagnostic blue color, commonly called "Denver Blue."

There are two separate deposits of alluvial sediments in the vicinity of the DFC. The Verdos Alluvium of Pleistocene age is a poorly sorted, stratified gravel containing lenses of sand, silt, and clay. In some drainages, the Denver Formation may be overlain by the Piney Creek Alluvium, well-stratified, interbedded organic sands, silts and clays with interbedded gravels.

Groundwater at the site generally moves from west to east and the average hydraulic velocity is about 30 cm per day in the upper alluvium and weathered Denver formation (McMahon et al., 1999). It is contaminated with volatile organic compounds, primarily TCE, cis-DCE, trichloroethane (TCA) and 1,1-dichloroethene(DCE). At the eastern boundary of the site, maximum concentrations of TCE, cis-DCE, TCA, and DCE were about 700 ppb, 360 ppb, 200 ppb and 230 ppb, respectively (FHWA, personal communication, 2002). At least one source of these VOCs was a leaking underground storage tank located near Building 52 that was used by the Federal Highway Administration (FHWA) to store waste, primarily TCA.

Groundwater flow from the aquifer discharges into McIntyre Gulch (Figure 2). McIntyre Gulch is a deep channel that penetrates the aquifer along the southern edge of the contaminant plume. Downing Reservoir is too shallow to be influenced by the aquifer, but the reservoir stage does affect the ground-water level.

In the fall of 1996, FHWA and GSA installed a permeable reactive barrier at the eastern edge of the DFC property along north-south trending Kipling Street (Figure 2). In contrast to the continuous wall design used at Elizabeth City, the DFC PRB has a funnel-and-gate design configuration. The funnel component of the PRB employs metal sheet pile that was driven into unweathered bedrock of the Denver Formation or into resistant, weathered layers of the Denver Formation. The depth of penetration of the funnel ranged from about 7.0 to 10 m. The PRB has 4 reactive gates, each 12.2 m long, up to 9.5 m deep, and from 1.8 m to (Gate 1) to 0.6 m (Gates 3 and 4) wide. The design thickness varied because of anticipated differences of contaminant fluxes to the PRB at different locations.

Table 1 provides a general comparison of the PRBs at Elizabeth City and the Denver Federal Center.

## **Methods**

### **Groundwater Sampling**

Groundwater was sampled from monitoring wells using peristaltic or submersible centrifugal pumps. At the USCG-SC, 10-2" PVC compliance wells have been monitored on a quarterly basis since November 1996 and up to 125 multi-level wells have been sampled on an annual basis since November 1996. At the DFC approximately 18 wells were sampled on an annual basis over the course of this study (1999-2000). Pumping rates were always between 150 and 250 mL/min to minimize chemical and hydrological disturbances in and around the well (Puls and Powell, 1992). Prior to sample collection, waters were pumped through a flow-through cell containing calibrated electrodes for pH, oxidation-reduction potential (ORP), specific conductance, and dissolved oxygen. Stabilization of electrode readings was assumed after 3 successive readings within  $\pm 0.10$  units for pH,  $\pm 10$  mV for ORP,  $\pm 3\%$  for specific conductance, and  $\pm 10\%$  for dissolved oxygen. After stabilization of electrode read-outs, turbidity was generally less than 5 NTUs. Filtered samples for cation analyses were collected using 0.45  $\mu\text{m}$  cartridge filters (Gelman aquaprep). Analyses were made using a Perkin Elmer Optima 3300 DV inductively coupled plasma spectrometer (ICP-OES). Anion samples were unfiltered and unacidified and analyses were carried out using capillary electrophoresis (Waters Quanta 4000E).

Colorimetric techniques were used in the field for Fe(II), dissolved oxygen, and hydrogen sulfide. Ferrous iron and sulfide were determined using the 1,10 phenanthroline and methylene blue indicators, respectively, and a HACH DR2010 spectrometer. Dissolved oxygen was measured using CHEMets test kits that employ the rhodazine D (low range) and indigo carmine (high range) colorimetric indicators. Alkalinity titrations were conducted in the field by titration with standardized sulfuric acid to the bromcresol green-methyl red endpoint. Dissolved  $\text{H}_2$  analyses were performed at the Denver Federal Center using the bubble strip method (Chapelle et al., 1997).

### **Core Collection and Analysis**

To assess the extent of corrosion and mineral buildup on the iron surfaces, 5 cm i.d. cores were collected using a Geoprobe™. Core barrels were driven using a pneumatic hammer to the desired sampling location and continuous, up to 110 cm, sections

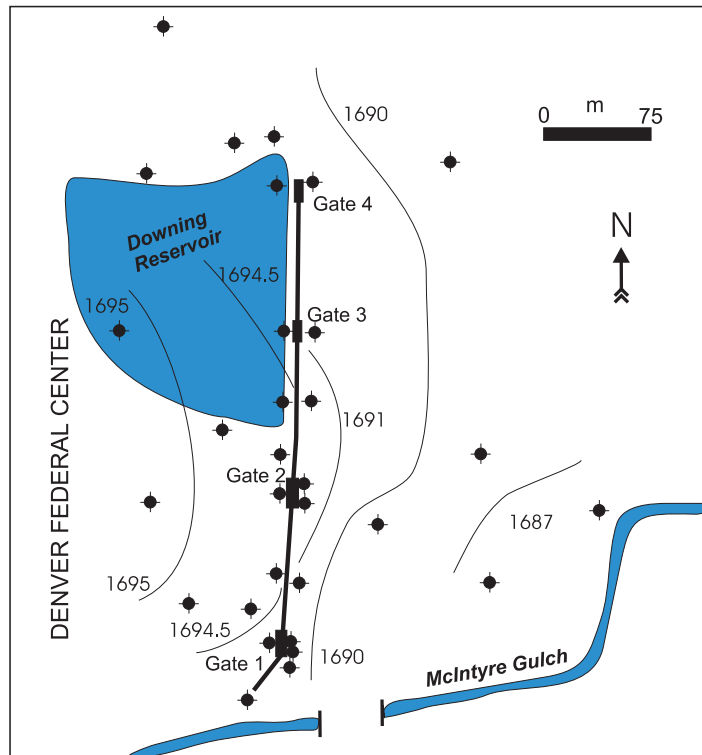


**Figure 2.** Plan view of Denver Federal Center PRB and groundwater elevations (after McMahon et al., 1999).

**Table 1.** Comparison of PRBs Investigated in this Study

Contaminants	PRB Configuration	Date Installed	Iron Dimensions	Iron Volume	Ground water, SC ( $\mu\text{S/cm}$ )	Groundwater, pH	Groundwater, DO (mg/L)
U.S. Coast Guard Support Center Cr(VI) TCE, cis-DCE	Continuous wall	6/96	46 m length 7.3 m deep 0.6 m wide	201 m <sup>3</sup>	325±126 (n=15)	5.94±0.44 (n=15)	0.5±0.4 (n=11)
Denver Federal Center TCE, TCA, cis-DCE	Funnel-and-gate	10/96	Gate 1 12.2 length 8.5 m deep 1.8 m wide	Gate 1 187 m <sup>3</sup>	Gate 1 1236±65 (n=3)	Gate 1 7.14±0.15	Gate 1 0.5±0.2
			Gate 2 12.2 length 9.5 m deep 1.2 m wide	Gate 2 139 m <sup>3</sup>	Gate 2 1358±10 (n=3)	Gate 2 7.19±0.08	Gate 2 0.2±0.1
			Gate 3 12.2 length 7.3 deep 0.6 m wide	Gate 3 53 m <sup>3</sup>	Gate 3 1306±10 (n=2)	Gate 3 7.06±0.07	Gate 3 <0.05

Notes: Geochemical parameters from Elizabeth City are average values ( $\pm 1$  s.d.) from upgradient monitoring well MW48. All parameters monitored quarterly since 2/97 to 3/01. Geochemical parameters from DFC gates 1, 2, and 3 are average values from wells GSA21, GSA26, and GSA31. Gate 1 and 2 parameters were measured on a yearly basis from 5/99 to 7/01, and gate 3 from 7/00 to 7/01. Information for DFC gate 4 is not included here; only gates 1-3 were studied in this investigation.

of iron, iron + soil, or iron + pea-gravel were retrieved. Angle cores (30° relative to vertical) and vertical cores were collected in order to assess the spatial distribution of mineral/biomass buildup in the reactive media. Prior to pushing the core barrel, an electrical conductivity profile was collected to verify the exact position of the iron/aquifer interface (e.g., Beck et al., 2001). In all cases core recovery was 60 to 85% of the expected value. Core materials from Elizabeth City and the Denver Federal Center (1999-2000) were broadly similar in appearance. In all cases the iron particles were jet black in color without any obvious signs of cementation or oxidation. Iron grains from the upgradient interface of DFC gate 2 were noticeably enriched in a black-colored, gel-like material. Immediately after collection the cores were frozen and shipped back to the Subsurface Protection and Remediation Division in Ada, Oklahoma, for sub-sampling and analysis. The frozen cores were partially thawed and then placed in an anaerobic chamber with a maintained H<sub>2</sub>-N<sub>2</sub> atmosphere. Each core was logged and partitioned into 5 to 10 cm segments. Each segment was homogenized by stirring in the glove box and then split into 4 sub-samples: (1) inorganic carbon analyses, (2) sulfur analyses/X-ray diffraction (XRD), (3) Scanning electron microscopy (SEM)/X-ray photoelectron spectroscopy (XPS) analyses, and, (4) microbial assays (phospholipid fatty acids, PLFA). All sub-samples were retained in airtight vials to prevent any air oxidation of redox-sensitive constituents.

Inorganic carbon analyses were conducted using a UIC carbon coulometer system. Weighed samples were placed in a glass reaction vessel and purged with CO<sub>2</sub>-scrubbed air. The samples were then acidified with hot, 5% perchloric acid and evolved CO<sub>2</sub> gas was carried to the coulometer cell containing a CO<sub>2</sub>-sensitive ethanolamine solution and quantitatively titrated. Hot, dilute perchloric acid dissolves carbonate precipitates such as siderite, calcite, aragonite, and carbonate forms of green-rust. The perchloric acid extraction does not liberate carbide-carbon, which is present at concentrations near 3 wt% in Peerless iron. Unreacted Peerless iron contains 15±5 ppm of acid extractable carbon. Total sulfur measurements were made with a UIC sulfur coulometer system. Iron samples were covered with V<sub>2</sub>O<sub>5</sub> and combusted in the presence of oxygen at 1050 °C. Evolved gases are passed through a column of reduced Cu to quantitatively convert all sulfur to SO<sub>2</sub>, which is then carried to the coulometer

cell where it is absorbed and coulometrically titrated. Un-reacted Peerless iron contains 5±1 ppm of sulfur using this combustion method. In addition, acid-volatile sulfide (AVS) and chromium-reducible sulfide (CRS) extractions were performed using hot, 6 M HCl and 1 M CrCl<sub>2</sub> in 0.5 M HCl, respectively (Zhabina and Volkov, 1978). These acid extractions determine the quantities of metal monosulfide precipitates (AVS) and iron disulfide precipitates (i.e., pyrite; CRS).

XPS measurements were made using a PE Model 5500 X-ray photoelectron spectrometer, operated with an Al Kα X-ray source at a power of 400 W (T. Sivavec, General Electric, Research and Development). Atomic concentrations were obtained from peak areas using established sensitivity factors. Depth profiles were measured by rastering a 4 kV argon beam over an area of 2x2 mm. X-ray diffraction patterns were collected of the fine-grained materials removed by sonication from the iron grains. Samples were mounted on a quartz plate and diffraction patterns were obtained using a Rigaku Miniflex diffractometer using Cu Kα radiation (0.01 degree step, 0.5 degrees two-theta per minute). Scanning electron and optical microscopy were utilized to determine the thickness of surface precipitates and evaluate physical morphology of grains and extent of surface coverage. Prior to microscopic characterization, samples were set in epoxy resin, cured, and ground and polished using standard techniques. Samples were analyzed for content and distribution of phospholipid fatty acids (PLFA; Microbial Insights, Inc.). PLFA analyses are based on the extraction and separation of lipid classes, followed by quantitative analysis using gas chromatography/mass spectrometry (GC/MS).

## Results and Discussion

### Groundwater Chemistry

Major anion and cation compositions of groundwater collected upgradient from the iron treatment zones at Elizabeth City and the Denver Federal Center are shown in Figure 3. Groundwater from Elizabeth City contains lower concentrations of total dissolved solids (<400 mg/L) compared to groundwater from the DFC (1000-1200 mg/L). At both sites, the concentration of dissolved oxygen in upgradient groundwater is about 1 mg/L and pH is near-neutral. There are, however, spatial variations in Eh values

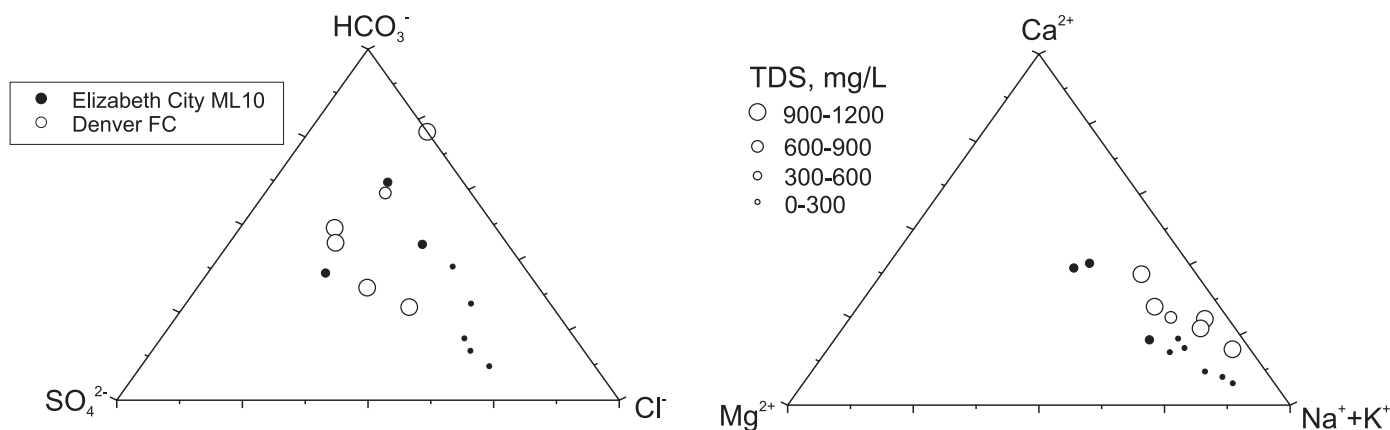


**Figure 3.** Upgradient groundwater compositions (molar ratios) and TDS values for the Elizabeth City and Denver Federal Center PRB sites.

of groundwater entering the iron zones at both sites (Table 2). Reactions between zero-valent iron and groundwater impact, to some extent, the concentration of all major solute species (Figure 4). Long-term trends indicate consistent removal of TCE and Cr(VI) at Elizabeth City as well as, among other species, sulfate, calcium, magnesium, and silica (Figure 4). Similar trends are observed at the DFC and are consistent with the patterns observed at other zero-valent iron PRB sites (Phillips et al., 2000; Liang et al., 2000; Battelle, 2000; Morrison et al., 2001). In downgradient wells, an analysis of data collected over five years at Elizabeth City shows little variation for most species; however, there are subtle time-dependent increases in pH and decreases in Eh (Figure 5).

A comparison of groundwater chemistry between upgradient and downgradient wells indicates that the iron zones at Elizabeth City and the DFC are long-term sinks for C, S, Ca, Si, Mg, N, and Mn. Concentrations of dissolved iron are elevated in downgradient compliance wells at Elizabeth City (Figure 5). Dissolved iron is not released from the zero-valent iron but probably from the downgradient aquifer due to decreased redox potentials in regions immediately downgradient from the iron media. In the region immediately upgradient from the iron wall at Elizabeth City, increases in the concentration of ferrous iron have led to the development of a reducing zone where a fraction of the hexavalent chromium is removed from the groundwater plume (Figure 4). Removal of chromium continues as the plume passes through the iron media.

### Reaction Path Modeling

Thermodynamic modeling can in principle be used as a predictive tool for estimating the types and quantities of mineral precipitates that form as groundwater reacts and approaches thermodynamic equilibrium with Fe<sup>0</sup> (Gavaskar et al., 1998; Blowes and Mayer, 1999; Morrison et al., 2001). The Geochemist's Workbench

program was used to simulate the incremental dissolution of Fe<sup>0</sup> into representative groundwater compositions from Elizabeth City and the DFC. The primary thermodynamic database was modified to include solubility data and reaction stoichiometry for zero-valent iron, iron monosulfides, and green-rusts (Table 3). Figure 6 shows the predicted changes in masses of minerals that precipitate and dissolve as the systems approach equilibrium with Fe<sup>0</sup>. In general, equilibrium modeling predicts that Fe<sup>0</sup> will eventually react to form magnetite, mackinawite, magnesium silicate, and/or magnesium hydroxide. Carbonates (calcite, dolomite), pyrite, quartz, and green-rust are predicted to be intermediate products. Although dolomite formation is predicted based upon equilibrium modeling, the precipitation of dolomite is unlikely in a PRB. Dolomite has a chemical formula CaMg(CO<sub>3</sub>)<sub>2</sub> and a crystallographic structure similar to that of calcite. It is well known that reactions to precipitate or dissolve dolomite are extremely slow at low temperatures (Hsü, 1967) so that dolomite precipitation is an unlikely cause of the comparatively rapid accumulation of inorganic carbon and magnesium in PRBs.

Interestingly, the reaction path model predicts the formation of carbonate-green-rust prior to magnetite, consistent with iron corrosion studies (McGill et al., 1976; Bonin et al., 2000). Green-rusts are unstable, mixed valence Fe(II)-Fe(III) hydroxy-salts that are highly susceptible to oxidation in the presence of oxygen. They are known to be transient products of iron corrosion that precipitate as metallic iron oxidizes to form Fe(III) oxyhydroxides (McGill et al., 1976; Schwertmann and Fechter, 1994). The structure of green-rusts consists of sheets of Fe(II)(OH)<sub>6</sub> in which some of the Fe(II) is substituted for by Fe(III). This mixture of ferrous and ferric iron results in a net positive layer charge, which is balanced by interlayer incorporation of anions such as Cl<sup>-</sup>, CO<sub>3</sub><sup>2-</sup>, and SO<sub>4</sub><sup>2-</sup>. Sulfate and carbonate forms of green-rust appear to be the most important in natural systems (e.g., Génin et al., 2001).

**Table 2.** Groundwater Chemistry at Elizabeth City (June, 2000; Median Values Transect 2) and the Denver Federal Center (July, 2000; Median Values)

	Elizabeth City aquifer		DFC – gate 1 aquifer		DFC – gate 2 aquifer	
		Fe <sup>0</sup>		Fe <sup>0</sup>		Fe <sup>0</sup>
pH	5.84	9.51	7.24	10.30	7.80	9.90
Eh (mV)	491	-347	233	-247	281	-35
O <sub>2</sub> (mg/l)	0.3	0.1	0.92	0.1	0.3	0.1
H <sub>2</sub> (nM)	---	---	0.63	948	2.38	304
Na (mg/l)	50	29	179	184	167	248
K	3.0	3.1	0.39	0.60	0.27	0.95
Mg	9.1	3.2	18.1	3.9	31	61
Ca	16.4	5.3	100	1.2	114	4.1
Fe	<0.04	0.05	0.19	<0.04	<0.04	<0.04
Sulfate	49	<1.0	234	<1.0	286	359
Chloride	51	25	52	59.7	66	83
Nitrate	0.9	<0.1	3.2	<0.10	2.9	1.1
Silica	10.9	<0.2	13.2	0.3	14.8	0.3
DIC	15	8	86	60	95	46
DOC	1.2	0.9	2.3	1.8	1.6	3.3
TDS	290	143	1090	510	1172	1011

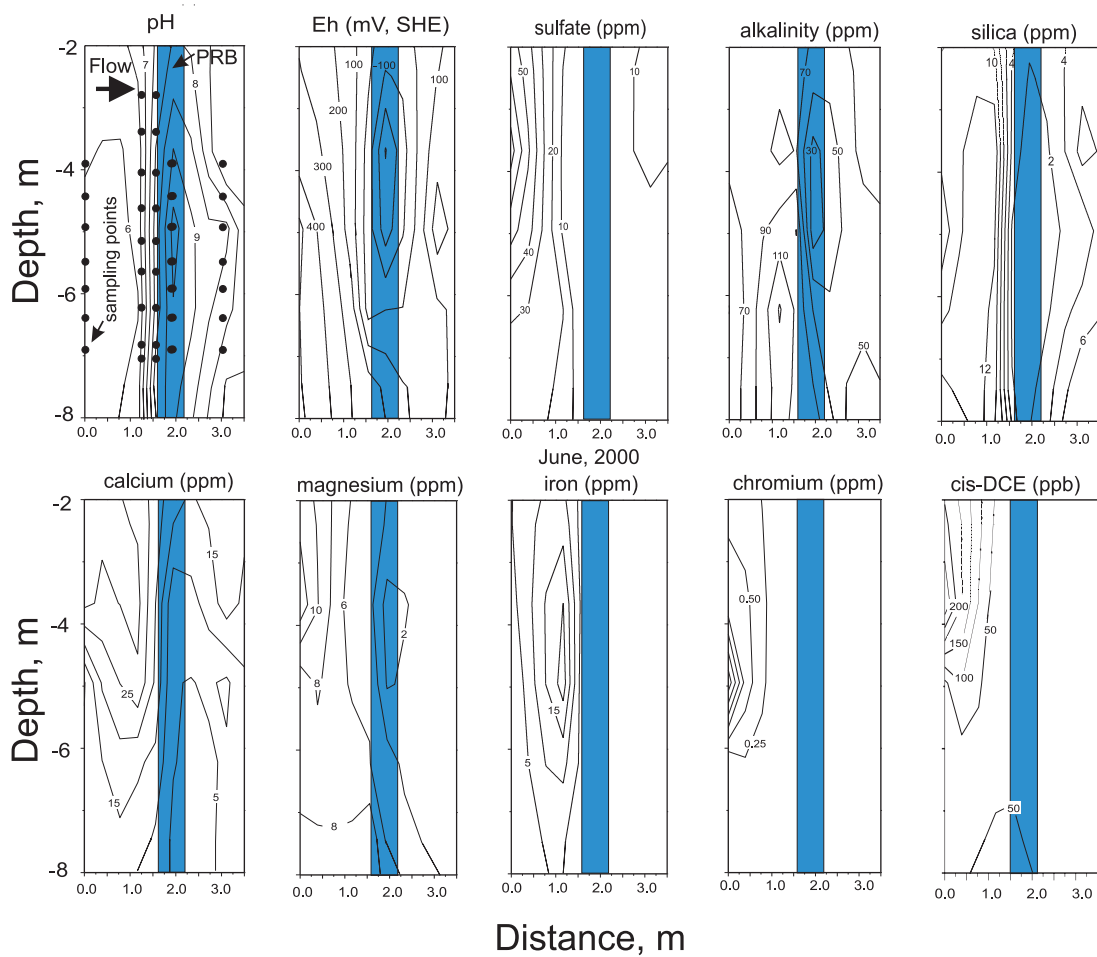


**Figure 4.** Cross-sectional profiles at the Elizabeth City PRB for selected species (June, 2000; Transect 2).

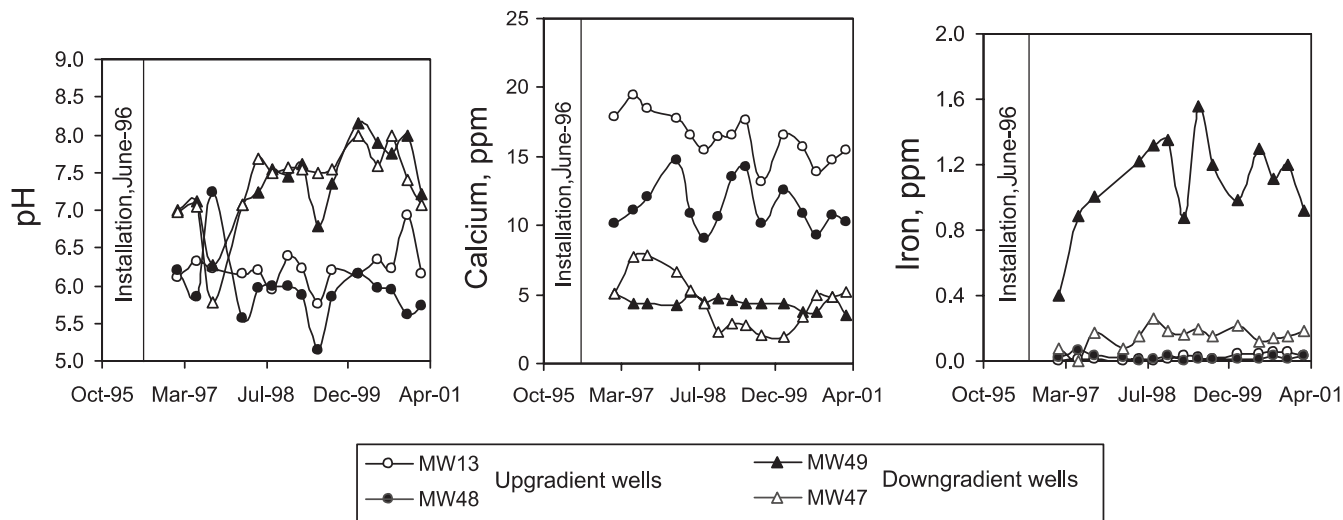


**Figure 5.** Time-dependent pH values and concentrations of calcium and iron in compliance wells from Elizabeth City (MW13, 30 m upgradient of PRB, screened interval 4.3-7.3 m; MW48, 0.6 m upgradient, screened interval 4.3-7.3 m; MW49, 1.8 m downgradient, screened interval 4.3-7.3 m; MW47, 1.8 m downgradient, screened interval 4.3-7.3 m).

**Table 3.** Thermodynamic Constants Added to the Geochemist's Workbench Database (Bethke, 1998)

Phase	Gibbs free energy of formation ( $\Delta G^\circ_f$ , kJ/mol)	Reference
Fe <sup>0</sup>	0	
Mackinawite (ordered)	-88.4	Benning et al. (2000)
Mackinawite (precipitated)	-83.7	Benning et al. (2000)
Green Rust SO <sub>4</sub>	-3785.0	Bourri� et al. (1999)
Green Rust Cl	-2145.0	Bourri� et al. (1999)
Green Rust CO <sub>3</sub>	-3588.0	Bourri� et al. (1999)
<i>Reactions</i>		
$\text{FeS} + \text{H}^+ = \text{Fe}^{2+} + \text{HS}^-$		
$\text{Fe}_6(\text{OH})_{12}\text{SO}_4 + 12\text{H}^+ = 4\text{Fe}^{2+} + 2\text{Fe}^{3+} + \text{SO}_4^{2-} + 12\text{H}_2\text{O}$		
$\text{Fe}_6(\text{OH})_{12}\text{CO}_3 + 12\text{H}^+ = 4\text{Fe}^{2+} + 2\text{Fe}^{3+} + \text{CO}_3^{2-} + 12\text{H}_2\text{O}$		
$\text{Fe}_4(\text{OH})_8\text{Cl} + 8\text{H}^+ = 3\text{Fe}^{2+} + \text{Fe}^{3+} + \text{Cl}^- + 8\text{H}_2\text{O}$		

Unfortunately, progress along the reaction path is arbitrary; the x-axes in Figure 6 do not represent time or space. Reaction path models may be used to qualitatively evaluate materials that might form in a PRB from an initial groundwater composition. However, with respect to predicting the space- or time-dependent accumulation of mineral mass or volume, reaction path modeling is less useful because it does not account for reaction rates or non-equilibrium processes (i.e., microbiological activity). Numerical models that consider kinetic limitations are beginning to provide reasonably accurate predictions of mineral accumulation in PRBs (e.g., Mayer et al., 2001), although there is still a need to collect field data to verify and refine these multicomponent reactive transport simulations.

### **Mineral Precipitates**

Solid-phase characterization studies implementing XRD, SEM-EDX, reflected-light microscopy, transmitted-light microscopy, XPS, and chemical extractions indicate the accumulation of lepidocrocite, magnetite, carbonate minerals (aragonite, siderite, or green-rust), and iron monosulfide as primary precipitates in the Elizabeth City and DFC PRBs. Similar authigenic precipitates in other Fe<sup>0</sup> PRBs were reported in previous field and laboratory studies (e.g., Phillips et al., 2000). The formation of these minerals is predictable based on the results of thermodynamic models discussed above. However, as previously noted, these equilibrium models are not able to successfully predict the rate of mineral buildup or the position of precipitates within the reactive media, both essential to understanding the impact of mineral precipitation on long-term remedial performance.

XPS scans show that iron particle surfaces from Elizabeth City and the DFC contain C, O, Fe, Si, S, Mg, Ca, Mn, and N. The XPS data indicate a surface layer dominated by iron oxyhydroxides, an intermediate layer of iron oxide, and finally zero-valent iron at the greatest sputtering depths. Surface carbon is present as carbonate with some detected hydrocarbon (binding energy 284.6 eV). The oxidation state of sulfur is predominantly present as sulfide (-2) but with minor amounts of sulfate (+6). Surface enrichment in the elements Ca, Mg, S, and Si are consistent with observed decreases in groundwater concentrations of these elements. Chromium was sometimes detected by XPS in iron samples from Elizabeth City, consistent with the reduction/precipitation mechanism for chromium uptake (Cantrell et al., 1995; Powell et al., 1995; Pratt et al., 1997). Table 4 lists the elements that preferentially partition to the iron media at Elizabeth City and the Denver Federal Center, the form of each element as it is transported to the iron media, and the possible solid-phase form of each element in the iron media. Research is continuing to identify the structure and mineralogy of precipitates that form near the surfaces of iron particles in the PRBs at Elizabeth City and the Denver Federal Center.

Microscopic observations indicate that mineral accumulation is mainly occurring on the surfaces of the iron particles where steep gradients in pH and redox potential promote mineral precipitation (Figure 7). After 3.5 years of mineral accumulation, a consistent coverage of surface material ranging in thickness from 10 to 50  $\mu\text{m}$  is observed on iron grains collected near the upgradient interface at Elizabeth City (horizontal penetration <8 cm). At greater penetration depths (>8 cm), surface coatings are

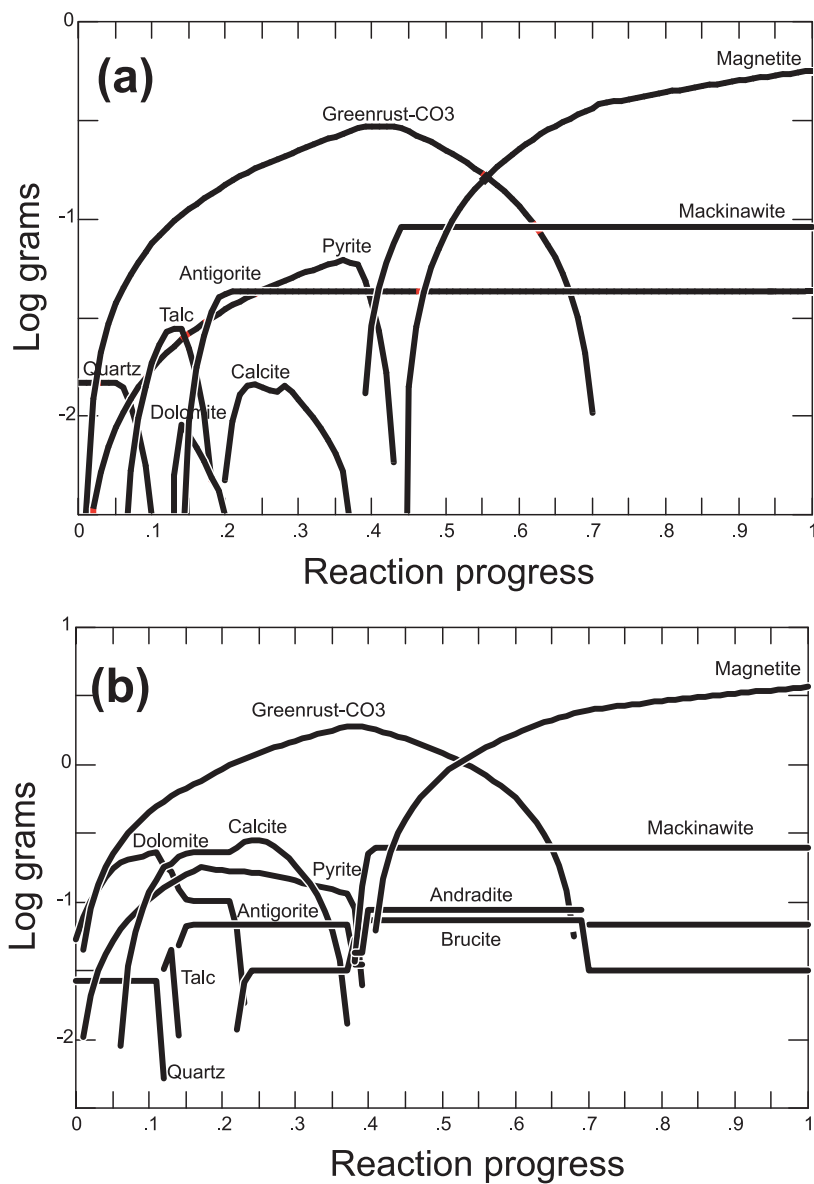


**Figure 6.** Reaction path model results showing mineral precipitation trends for representative groundwater compositions from (a) Elizabeth City and (b) Denver Federal Center (gate 2).

**Table 4.** Elements Removed from Groundwater by Fe<sup>0</sup> PRBs, Input Forms, and Possible Solid Phase Associations

element	input form	solid phase association
C	HCO <sub>3</sub> <sup>-</sup>	CaCO <sub>3</sub> , FeCO <sub>3</sub> , Fe <sub>6</sub> (OH) <sub>12</sub> CO <sub>3</sub>
S	SO <sub>4</sub> <sup>2-</sup>	FeS
Ca	Ca <sup>2+</sup>	CaCO <sub>3</sub> , sorbed (?)
Mg	Mg <sup>2+</sup>	incorporation into CaCO <sub>3</sub> ; Mg-OH-Si ppts (?)
Si	H <sub>4</sub> SiO <sub>4</sub> <sup>0</sup>	sorbed onto Fe(OH) <sub>3</sub> (?)

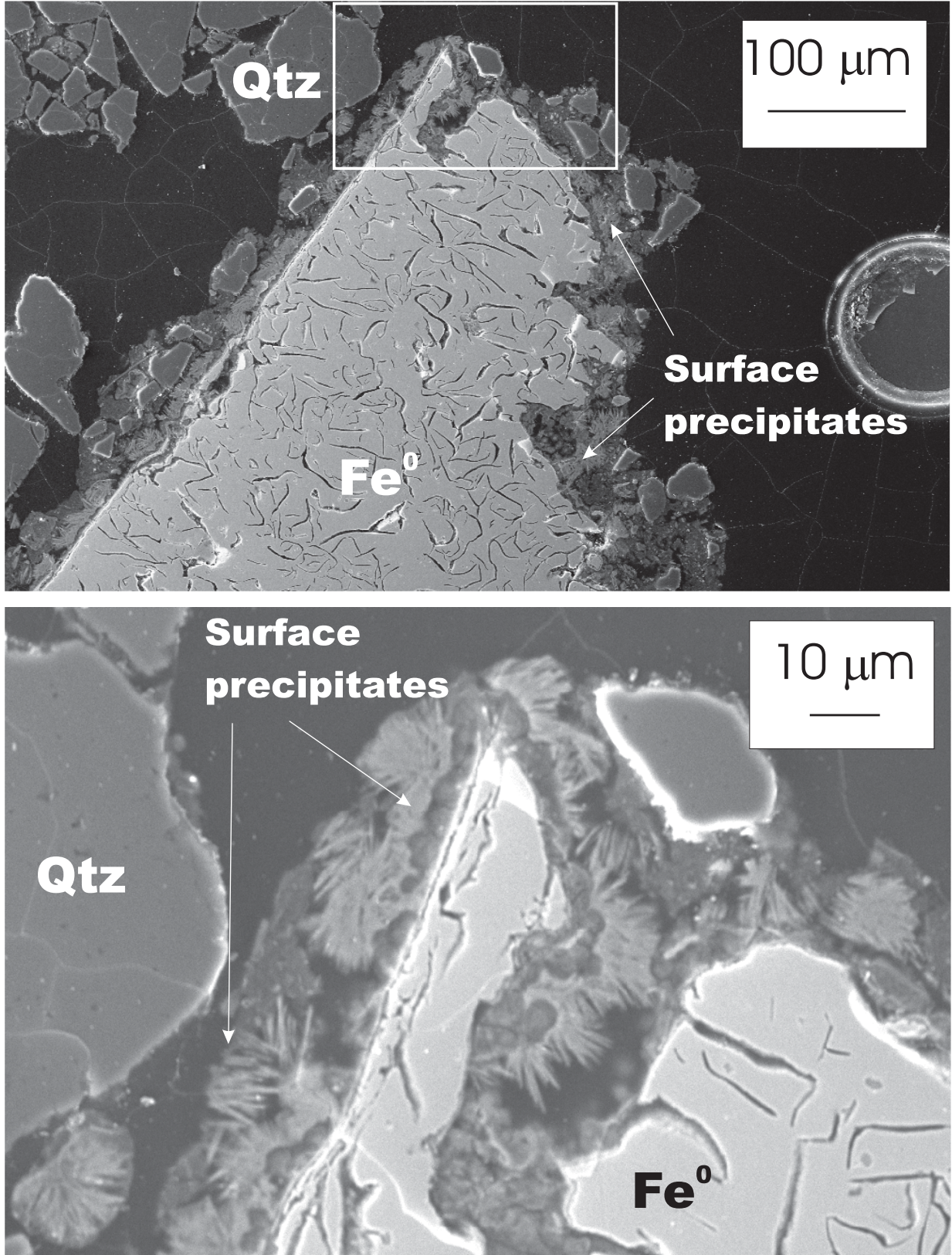


**Figure 7.** SEM photomicrographs of iron particles collected near the upgradient iron/aquifer interface (Elizabeth City, 2000).

discontinuous and <5  $\mu\text{m}$  thick. Where mineral accumulations are the greatest, distinctive particle morphologies include radiating needles, characteristic of carbonates formed at high degrees of supersaturation; homogenous crusts without euhedral morphologies, characteristic of iron oxyhydroxides; and thin coatings or aggregates of very fine-grained particles, characteristic of iron monosulfides. Textural forms and coating thickness of surface precipitates are broadly similar at the DFC and are comparable to those reported from the Y-12  $\text{Fe}^0$  barrier (Phillips et al., 2000).

Eighteen cores were analyzed to determine concentrations and spatial distribution of inorganic carbon (IC) and sulfur accumulation in the Elizabeth City and the DFC  $\text{Fe}^0$  PRBs. At both sites, accumulation of IC and sulfur is greatest near the upgradient soil- $\text{Fe}^0$  interface, with concentrations decreasing with increasing penetration into the iron (Figure 8). Anomalous buildup of mineral precipitates and microbial biomass is readily apparent in gate 2 of the DFC. Concentrations of IC in gate 2 are as high as 8000 ppm and total sulfur values approach 4500 ppm, or a factor of about 4x the amounts observed in DFC gate 1 or the Elizabeth City PRB.

Total sulfur measurements compare well with the results of acid-volatile sulfide (AVS) extractions (Figure 9). Sulfur in the reactive barrier system is mainly present as labile, iron sulfide phases. Iron sulfides could potentially enhance the degradation of halogenated aliphatic compounds in PRBs (Butler and Hayes, 2000). The high pH, low Eh geochemical signature in iron zones favors the chemical reduction of sulfate to sulfide. Rates of chemical sulfate reduction at low temperatures are extremely slow (Trudinger et al., 1985). It is expected, therefore, that the low Eh (high hydrogen fugacity) environment supports metabolism by sulfate-reducing bacteria in the iron (see Microbiology section below). Bisulfide respired by these bacteria rapidly reacts at high pH with ferrous iron produced via the dissolution of the zero-valent iron to form acid-volatile sulfides. Less than about 5% of the accumulated sulfur in the  $\text{Fe}^0$  is extractable with hot chromous chloride which suggests either that some transformation of the iron monosulfides to pyrite ( $\text{FeS}_2$ ) has occurred or that labile AVS phases have transformed to more crystalline, acid-resistant iron monosulfides (most likely greigite). The solubility of precipitated mackinawite decreases with increasing pH and can be described by:



with  $\log K_{\text{sp}} = -3.6$  (Benning et al., 2000). At pH 10 and  $\log a_{\text{Fe}^{2+}} = -5$  (typical of Elizabeth City water), the expected equilibrium activity of bisulfide is  $10^{-8.1}$ , which is much lower than the nominal detection limit of the methylene blue method ( $\sim 10^{-5.8}$  mol/L) for dissolved sulfide. Therefore, the detection of hydrogen sulfide in groundwater samples collected from  $\text{Fe}^0$  media is not necessarily an indicator of whether iron sulfides are precipitating in the reactive media. Concentrations of hydrogen sulfide up to 0.5 mg/L were observed in groundwater samples collected from the DFC. These high dissolved sulfide values suggest that particulates were entrained during well purging even at the low flow rates used in this study.

Porosity loss in the iron zones due to the precipitation of inorganic carbon and sulfur minerals was estimated by integrating the concentrations of IC and S as a function of distance in the iron and estimating the volume loss by using the molar volumes of pure calcite ( $\text{CaCO}_3$ ), siderite ( $\text{FeCO}_3$ ), and mackinawite ( $\text{FeS}$ ). The proportion of IC present as calcite and siderite was calculated by evaluating the excess drawdown of dissolved inorganic carbon

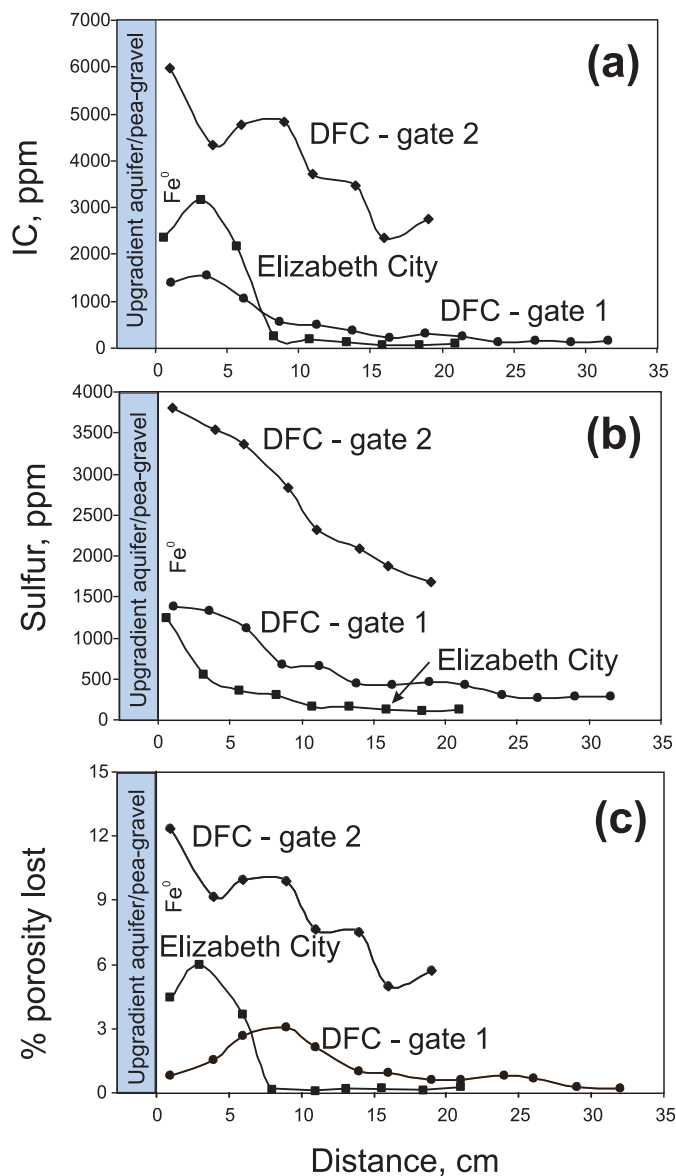


**Figure 8.** Concentration distribution of (a) solid phase inorganic carbon, (b) sulfur, and (c) calculated porosity lost after ~4 years in the  $\text{Fe}^0$  media at Elizabeth City and the DFC. Concentrations of C and S were obtained from cores EC060300-4 (Elizabeth City); C1-2-71000 (DFC, gate 1); and, C2-17-71300 (DFC, gate 2). Porosity lost is calculated with  $[(\text{initial porosity} - \text{final porosity}) / (\text{initial porosity})]$ .

relative to dissolved calcium concentrations between upgradient and downgradient monitoring wells. This method suggests that inorganic carbon is evenly distributed between  $\text{FeCO}_3$  and  $\text{CaCO}_3$  at Elizabeth City; the DFC gates are slightly enriched in  $\text{FeCO}_3$  (60%) relative to  $\text{CaCO}_3$  (40%). Porosity gain due to the dissolution of  $\text{Fe}^0$  was estimated by assuming that all  $\text{Fe}^{2+}$  released was precipitated as siderite and mackinawite. Because the cores were collected at an angle, the measured concentration profile

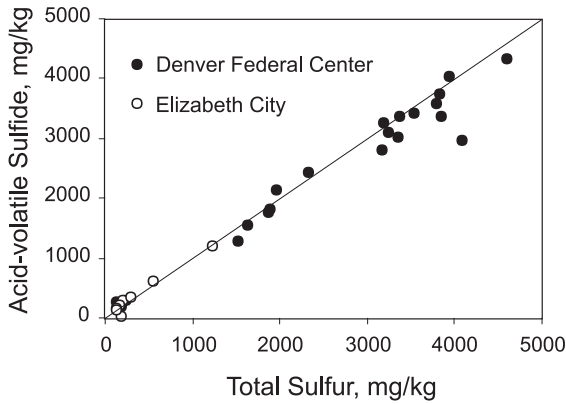


**Figure 9.** Total sulfur concentration versus acid-volatile sulfide concentration in the Fe<sup>0</sup> media at Elizabeth City and the DFC.

was adjusted to reflect horizontal penetration:  $x = \sin 30^\circ \cdot x'$ , where  $x'$  is the measured midpoint of each core sub-sample and  $x$  is the corrected distance, reflecting core penetration relative to a vertical plane along an axis parallel to flow. To calculate the total mass of mineral accumulation, we assume that concentration profiles are independent of position within the reactive media. The concentration (mg/kg) of IC precipitates, for example at Elizabeth City in June 2000, can be described by the exponential function:  $IC(x) = 1802.7 e^{(-x/12.16)}$  ( $r^2=0.97$ ). Similarly sulfur accumulation can be described by:  $S(x) = 1612.7 e^{(-x/16.38)}$  ( $r^2=0.95$ ). These equations are then integrated to evaluate the mass loading of IC and S, i.e.,

$$M_{IC} = \int_0^{x_i} (IC \cdot y \cdot z \cdot \rho) dx \quad (6)$$

Where  $x_i$  is the thickness of the iron zone,  $y$  is the height of the iron zone,  $z$  is the length, and  $\rho$  is the effective reactive media density, estimated to be  $2.72 \text{ g cm}^{-3}$  based on estimates of emplaced bulk density at Elizabeth City (Blowes et al., 1999a). Table 5 shows the results of the minerals accumulation calculations in terms of total mass and surface area-normalized accumulation.

A progressive increase in the mass of authigenic carbon and sulfur in the PRB at Elizabeth City is apparent from the data in Table 5. After 48 months of operation, the average rates of sulfur

and carbon accumulation at Elizabeth City are  $0.024 \pm 0.007 \text{ kg m}^{-2}\text{y}^{-1}$  and  $0.087 \pm 0.040 \text{ kg m}^{-2}\text{y}^{-1}$ , respectively. There is no apparent decrease in the uptake rate of these elements after four years of operation. Based on the data presented in Table 5, the highest mass flux values of this study are found in gate 2 of the DFC. The mass flux of IC in gate 2 is about an order of magnitude greater than that in gate 1. The mass flux of sulfur accumulating in gate 2,  $0.803 \text{ kg m}^{-2}\text{y}^{-1}$ , is broadly comparable to recently determined sulfur flux in a compost subsurface reactive barrier,  $1.47 \text{ kg S m}^{-2}\text{y}^{-1}$  (Herbert et al., 2000).

The total volume associated with the IC and S authigenic precipitates is listed in Table 5 assuming that the precipitates were evenly distributed over all iron surfaces (see discussion of this assumption below). Assuming an initial porosity of 50% in the iron walls at Elizabeth City, the net annual porosity loss associated with the formation of IC and S precipitates and the dissolution of Fe<sup>0</sup> is estimated to be ~0.1% of the total available volume per year. If all mineral mass accumulates in the front 8 cm, the annual porosity loss is estimated to be 0.75%. This value is in good agreement with estimates based on the results of combined chemical reaction and groundwater transport modeling, e.g., Blowes and Mayer (1999) estimate that after 20 years, porosity of the upgradient portion of the reactive iron will decrease from 50% to 30%, or that porosity will be lost at an average rate of about 1% per year. An annual porosity loss, 0.03%, is estimated for gate 1 at the DFC assuming that precipitates are evenly distributed throughout the entire wall; whereas, gate 2 shows an anomalous rate of porosity loss of 0.43% per year. This value can be compared with the value estimated by McMahon et al. (1999), 0.35% per year, determined by evaluating solute concentrations and the precipitation only of inorganic carbon as calcite and siderite.

Because the amount and rate of mineral accumulation and the rate of iron corrosion varies spatially, so does the rate of porosity infilling. Consequently, pore infilling models must account for the fact that the total mass of mineral precipitates is unevenly distributed within the PRB. The highest concentrations of mineral precipitates and rates of porosity loss are found adjacent to the upgradient interface (Figure 8). At Elizabeth City, a maximum volume loss of 5.9% is estimated at 2.5 cm into the iron media, but then decreasing to <0.1% at distances >8 cm. In gate 1 of the DFC, the precipitation front is spread out over a greater distance in the iron and may be the result of higher flow rates in gate 1 (0.38 m/d) compared to Elizabeth City (0.15 m/d). In gate 2, 14.2% of the available porosity in first 2.5 cm of iron was lost over the first 3.75 years of operation.

**Table 5.** Mass Accumulation of Inorganic Carbon and Sulfur and Estimated Annual Volume Loss

	date	mass IC (kg)	mass S (kg)	flux IC ( $\text{kg m}^{-2} \text{y}^{-1}$ )	flux S ( $\text{kg m}^{-2} \text{y}^{-1}$ )	V FeCO <sub>3</sub> ( $10^3 \text{ x cm}^3 \text{ y}^{-1}$ )	V CaCO <sub>3</sub> ( $10^3 \text{ x cm}^3 \text{ y}^{-1}$ )	V FeS ( $10^3 \text{ x cm}^3 \text{ y}^{-1}$ )	V loss (% total y <sup>-1</sup> )	
Elizabeth City	6/98	28.4	11.7	0.058	0.024	17.3	21.9	3.9	0.05	
	6/98	---	7.6	---	0.016	---	---	2.5		
	6/99	68.3	13.1	0.093	0.018	27.7	35.1	2.9	0.08	
	6/00	136.6	28.9	0.140	0.030	41.6	52.7	4.8	0.12	
	6/00	53.8	29.8	0.055	0.031	16.4	20.7	5.0	0.05	
DFC	gate 1	7/00	34.2	41.2	0.204	0.246	13.3	11.3	7.4	0.03
	gate 2	7/00	481.9	179.4	2.158	0.803	188.0	158.7	32.0	0.43

Note: V loss is the net annual porosity lost assuming that all precipitates accumulate evenly throughout the PRB.

Mass balance on C and S was estimated by evaluating solid phase concentration data and the changes in the groundwater concentrations of inorganic carbon and sulfate. Mass accumulation of IC and S in the Fe<sup>0</sup> media based on changes in groundwater solute concentrations was estimated from  $Q \cdot \Delta C$ , where  $Q$  is the volumetric flux of water through the iron media (L/y) and  $\Delta C$  is the change in the concentration of dissolved IC and S (mg/L) between upgradient and downgradient sampling points. Average groundwater flow velocities at Elizabeth City of 0.13 to 0.18 m/d were reported by Blowes et al. (1999). McMahon et al. (1999) report flow median velocities in gate 1 and gate 2 at the DFC of 0.38 m/d and 0.11 m/d, respectively, based on heat pulse flowmeter measurements. Results for carbon mass balance (Figure 10) agree to within a factor of 1.5x for the Elizabeth City PRB and gate 2 of the DFC, but with poor agreement in gate 1. Sulfur mass balance is in reasonable agreement for gates 1 and 2 of the DFC. Considerably more accumulation of sulfur is expected in the Elizabeth City PRB than has been observed on the core materials. In gate 2, more solid phase C and S is observed on the iron grains than is predicted from the observed changes in groundwater chemistry. These trends may indicate that rates of mineral accumulation have decreased with time, i.e., the estimates in Table 5 are based on the assumption of steady-state conditions throughout the lifetime of the PRBs. Several factors lead to uncertainty in the mass balance calculations for PRBs. Estimates of accumulation based on changes in groundwater chemistry depend on chemical and hydrogeologic measurements. Determination of dissolved constituents may be analyzed at a high level of accuracy and precision. However, estimates of the mass flux of ground water moving through PRBs are prone to large uncertainties. Estimates of accumulation based on characterization of core materials depend on analytical measurements and also on estimates of emplaced iron density. Spatial heterogeneity in groundwater flow velocity, concentration of solutes, concentration of solid phase products, and emplaced iron density all factor into the uncertainty analysis of mass balance calculations.

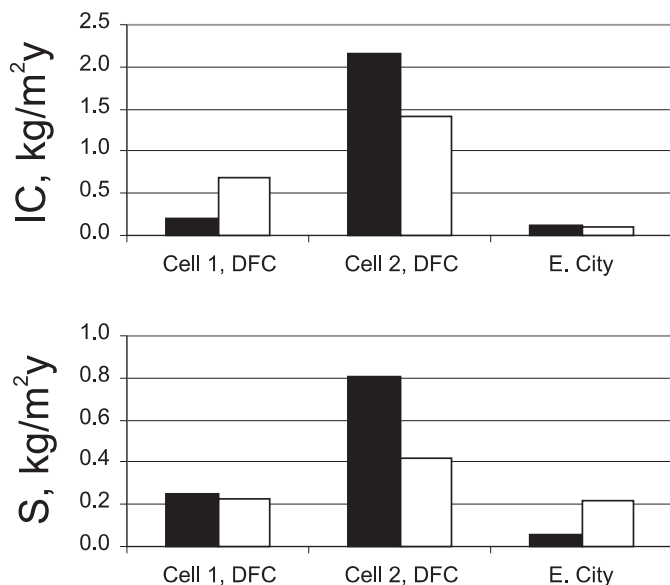


**Figure 10.** Mass balance estimate for inorganic carbon and sulfur in the Fe<sup>0</sup> media at Elizabeth City and the DFC. Solid bar based on solid-phase characterization; open bar based on groundwater composition and flow rate.

Several transformation pathways of iron minerals in Fe<sup>0</sup> PRBs are important to evaluations of long-term performance by affecting the surface properties and reactivity of the iron particles and reducing available porosity. Oxidized, reduced, and mixed-valence iron phases form and undergo transformation in Fe<sup>0</sup> systems. Oxidized phases (lepidocrocite, goethite) apparently are the result of reactions with dissolved oxygen; elevated DO concentrations can lead to rapid corrosion and clogging of Fe<sup>0</sup> due to ferric oxyhydroxide precipitate at the upgradient interface (Liang et al., 2000). Akaganéite has been identified based on X-ray diffraction analyses at the PRB from Y-12 plant site (Phillips et al., 2000). Akaganéite is rare in nature; its formation is restricted to Fe- and Cl-rich hydrothermal brines and as the result of iron corrosion in Cl-rich fluids. Akaganéite also forms as an alteration product of green-rust compounds (Schwertmann and Taylor, 1989) and therefore may be related to sample preservation and the oxidation of green-rust compounds rather than incipient precipitation of this phase as an iron corrosion product in groundwater systems.

Mixed valence state iron minerals include magnetite and green-rust compounds. Green-rust compounds are corrosion products that are expected to form under more reducing conditions than do iron oxyhydroxides. Their precipitation is favored under alkaline conditions and transformation of these compounds to magnetite is expected based on the thermodynamic calculations presented in a preceding section. Iron carbonate and monosulfides are the primary reduced iron forms and are likely to persist as long as reducing, alkaline conditions persist. Although iron monosulfides are unstable relative to pyrite, the kinetics of this transformation process decrease with increasing pH so that iron monosulfides may be the long-term solid phase sulfide in Fe<sup>0</sup> PRBs. Similarly, substantial iron carbonate dissolution is not expected so long as alkaline conditions persist. Research at EPA is continuing on the factors that govern iron mineral transformations in PRBs and impacts to system longevity and performance.

### Microbiology

Seventy-one core samples collected from the Elizabeth City and DFC PRBs were analyzed for content and distribution of phospholipid fatty acids (PLFA). These organic compounds can be used as lipid biomarkers to provide a quantitative means to evaluate viable microbial biomass, community composition, and nutritional status. The cores contained sediments from upgradient and downgradient locations adjacent to the PRBs, iron filings from the PRB matrix, or a mixture of sediment and iron matrix when the cores were collected at sediment/PRB interface. The highest accumulations of microbial biomass were found at the DFC in iron samples from gate 2. Concentrations as high as 4,100 pmoles/g dry wt were measured in iron matrix samples from approximately 17 ft below ground surface in gate 2 which is equivalent to  $8.36 \times 10^7$  cells per gram of iron matrix. Sediment samples from 0 to 5 cm upgradient of the gate 2 PRB had similar biomass levels and composition. Microbial biomass correlates well with total sulfur suggesting that the accumulated biomass contains anaerobic, sulfate-reducing bacterial consortia. The presence of this consortium is also supported by the analysis of PLFA structural groups that suggest the presence of sulfate-reducing bacteria (mid-chain branched saturate fatty acids; Dowling et al., 1986; Parkes et al., 1992), of Gram negative anaerobic bacteria (terminally branched saturate fatty acids; Parkes et al., 1992; Guckert et al., 1985), and of anaerobic metal-reducing strains (branched monoenic fatty acids; Parkes et al., 1992; Edlund et al., 1985). These three PFLA structural groups comprise approximately 30% of the total PFLA mass in gate 2 samples.

It is perhaps of value to compare the biomass and community structure information in gate 2 samples versus gate 1 samples due to differences in performance observed at these two PRB systems at the DFC (Table 6). The overall distribution of PLFA structural groups varies between gates 1 and 2. The higher biomass, % contribution of anaerobic bacteria, and bacteria to eukaryote ratio in gate 2 are all consistent with an anaerobic PRB environment with a higher biological energy sink, suggesting that hydrogen levels would be lower and that less reducing power would be available for chemical reduction (White et al., 1980). This would seem to agree with the lower dissolved hydrogen levels seen in gate 2 (Table 2), and with the breakthrough of contaminants due to less available reducing power and/or biomass impacting system hydraulics. The higher pH and lower Eh values associated with gate 1 would also create an environment less conducive to bacterial growth, although it is interesting to speculate as to the conditions that govern microbial growth and the conditions that are impacted by microbial growth.

The availability of 45 samples from the Elizabeth City PRB, collected as vertical, upgradient and downgradient interfacial cores, allows for some analysis of the spatial distribution of bacterial biomass and biomass composition. The highest biomass levels were observed in upgradient core subsections, which contained the sediment/iron interface (Figure 11). These samples contained from 600 to 900 pmoles of PLFA per gram of sediment and iron. This is equivalent to 1 to  $2 \times 10^7$  cells per gram of solid matrix or less than half the maximum detected in DFC samples from gate 2. While total biomass peaked at the sediment/iron interface, the contribution of anaerobic biomarkers identified above (TerBrSats, BrMonos, MidBrSats) as a percent of total biomass peaked 1 to 3 inches into the iron matrix (Figure 12). The localization of metal and sulfate reducing activity near the upgradient sediment/PRB interface would seem to correlate reasonably well with the iron, sulfate, and Eh contours shown in Figure 4, and with the sulfur concentrations and porosity changes illustrated in Figure 8. Evaluation of the microbial populations through the PLFA data from downgradient PRB/sediment interface is more difficult. As shown in Figure 13, no clear pattern of biomass distribution or population composition is immediately apparent, although there seems to be some enhancement of an anaerobic population immediately down stream of the interface. Microbial counts range from  $1.85 \times 10^6$  to  $2.51 \times 10^3$ , thus downgradient cores seem to contain a 10-fold reduction in the

range of values (at both the maximum and minimum) compared to the upgradient cores. The lower counts associated with the mid-barrier and downgradient samples suggest that the environment at these locations is more challenging to bacterial growth and survival. Examining the geochemical conditions associated with these locations supports this hypothesis. Figure 4 indicates a decrease in biologically available electron acceptors such as sulfate and cis-DCE in the mid-wall and downgradient locations. The higher pH along with precipitated iron and sulfur species would also tend to create a more severe environment for bacterial growth. Table 2 also suggests that mid-barrier and downgradient locations may be less conducive for growth due to a higher pH and a lack of electron acceptors (oxygen, sulfate, nitrate), which would seem to negate the positive influence of an abundant electron donor, dissolved hydrogen.

The use of cathodic hydrogen as an energy source for biofilm development has been a staple of the corrosion literature for some time (Von Wolzogen Kuehr and van der Vlugt, 1934). The high surface areas of PRBs and the supply of electrochemically active species such as sulfur oxyanions insure the development of dissolved hydrogen in the PRB and the local subsurface environment. Using the USCG-SC PRB as an example, we can conduct some theoretical exercises to evaluate the potential impact of biomass development on PRB performance based on direct geochemical measurements. Assuming that the PRB represents a 300 m<sup>2</sup> cross section, and has a flow of 0.15 m/day, 50 % porosity, and an average dissolved hydrogen level of 500 nm, the net hydrogen production would be 6.75 mmoles/day (Cord-Ruwish, 2000). This could yield 0.675 cm<sup>3</sup>/day (assuming 0.5 mol ATP/mol H<sub>2</sub>, 200 g Biomass/mol ATP, Biomass density 1g/cm<sup>3</sup>) and the Fe(II) concentrations in Figure 4 yield 24.2 cm<sup>3</sup>/day (assuming 1 mol Fe(II)/mol H<sub>2</sub>). While these estimates of biomass formation seem insignificant, the localization of this activity in discrete zones and interaction with inorganic precipitates may magnify the effect. However, the bio-available energy and thus potential biofilms generating capacity represented by the PRB is enormous. A 1 m<sup>2</sup> surface area that corrodes at 0.1 mm per year would yield, using a density of iron of 7800 kg/m<sup>3</sup>, 14 moles of H<sub>2</sub>/day or approximately 40 mmoles/day. This is equivalent to 1.5 μm of biomass per day over the entire surface area of the PRB. This assumes uniform growth and no loss to predation or sloughing of biomass. Nevertheless, these numbers indicate a significant potential for biofouling in PRBs.

**Table 6.** PLFA Results for DFC Gates 1 and 2

site	ave. biomass	cells/g	bact/euk ratio	% anaerobic
DFC gate 1	325	$6.5 \times 10^6$	156	~12%
DFC gate 2	2283	$4.6 \times 10^7$	>600	~30%

Notes: Average biomass in pmoles PLFA/g dry wt. Cell/g is estimated bacterial cells per gram dry weight of sample based on  $10^8$  pmoles PLFA per gram dry weight of cells and  $2.0 \times 10^{12}$  cells per gram dry weight cells. Bac/euk ratio is the average bacteria to eukaryote ratio, ratio of polyenoic PLFA to total- polyenoic PLFA. %Anaerobic is the percent of total PLFA composed of terminally branched fatty acids, branched monenoic fatty acids and mid-chain branched fatty acids. Values are average of 12 gate 1 samples or 14 gate 2 samples collected 7/2000.

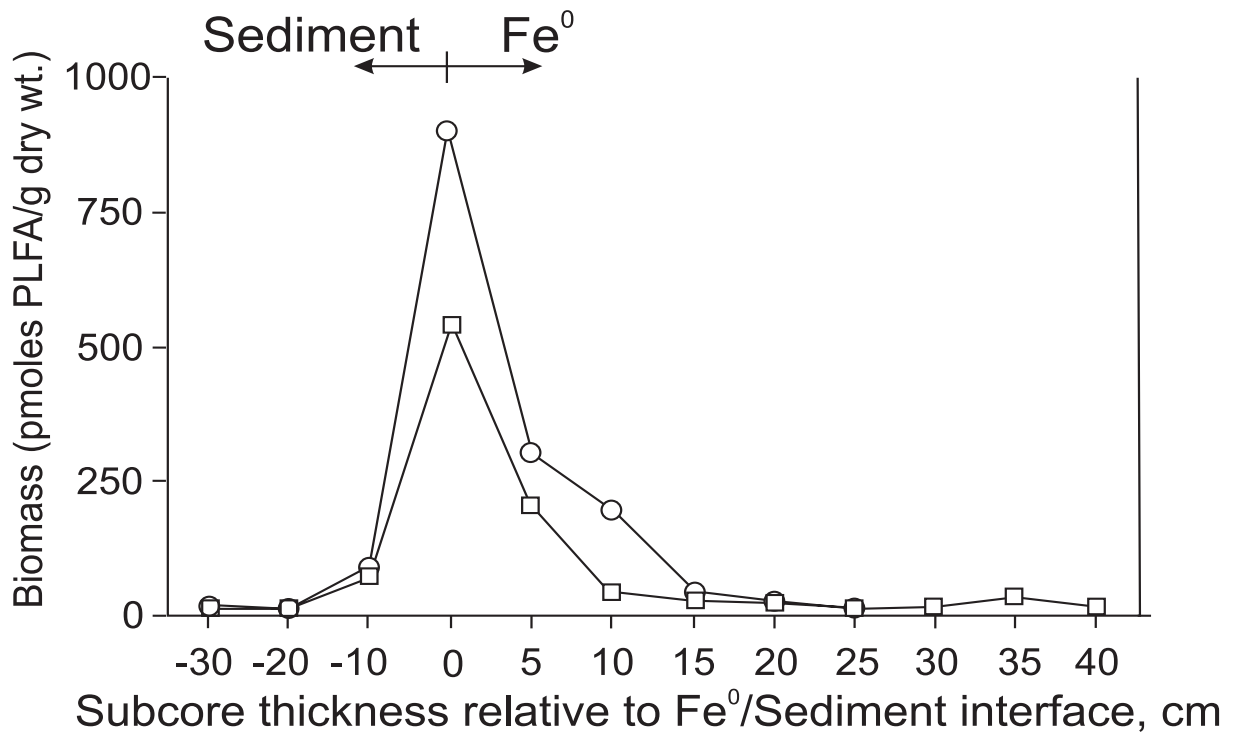


**Figure 11.** Biomass concentration in Elizabeth City cores collected June, 2000 (upgradient aquifer/iron region). PLFA data collected from core EC060200-1 (open circles) and core EC060300-4 (open squares).

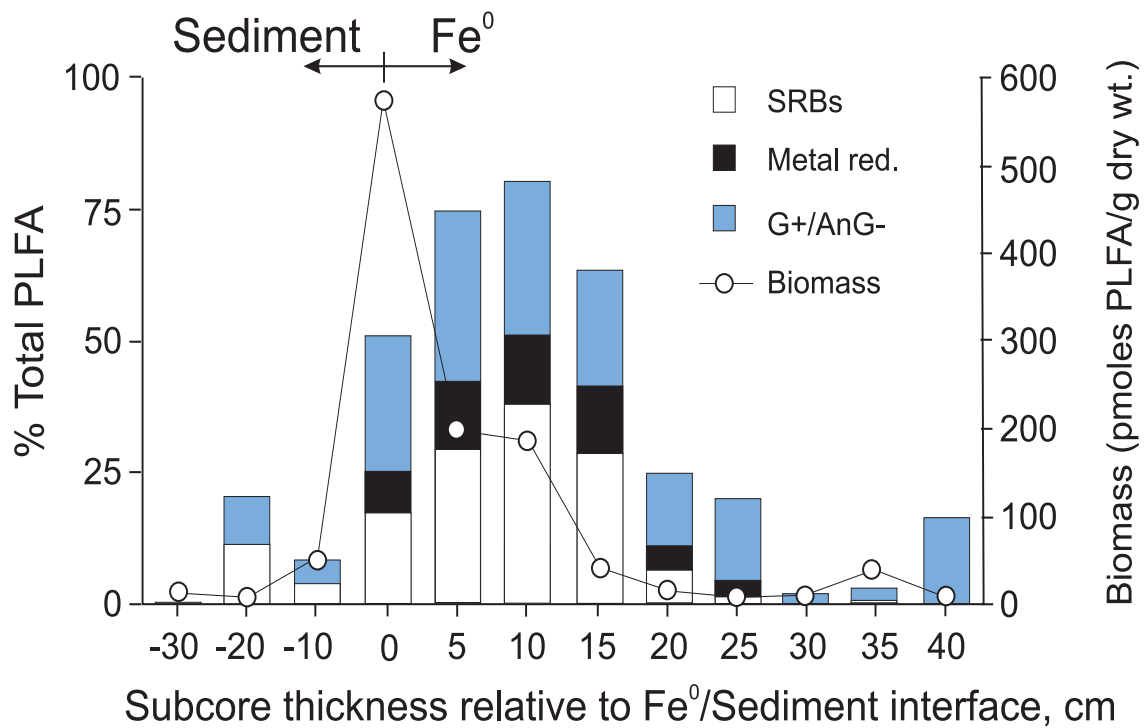


**Figure 12.** Concentration and distribution of PLFA in Fe<sup>0</sup> from Elizabeth City core EC060300-4 (upgradient aquifer/iron region).

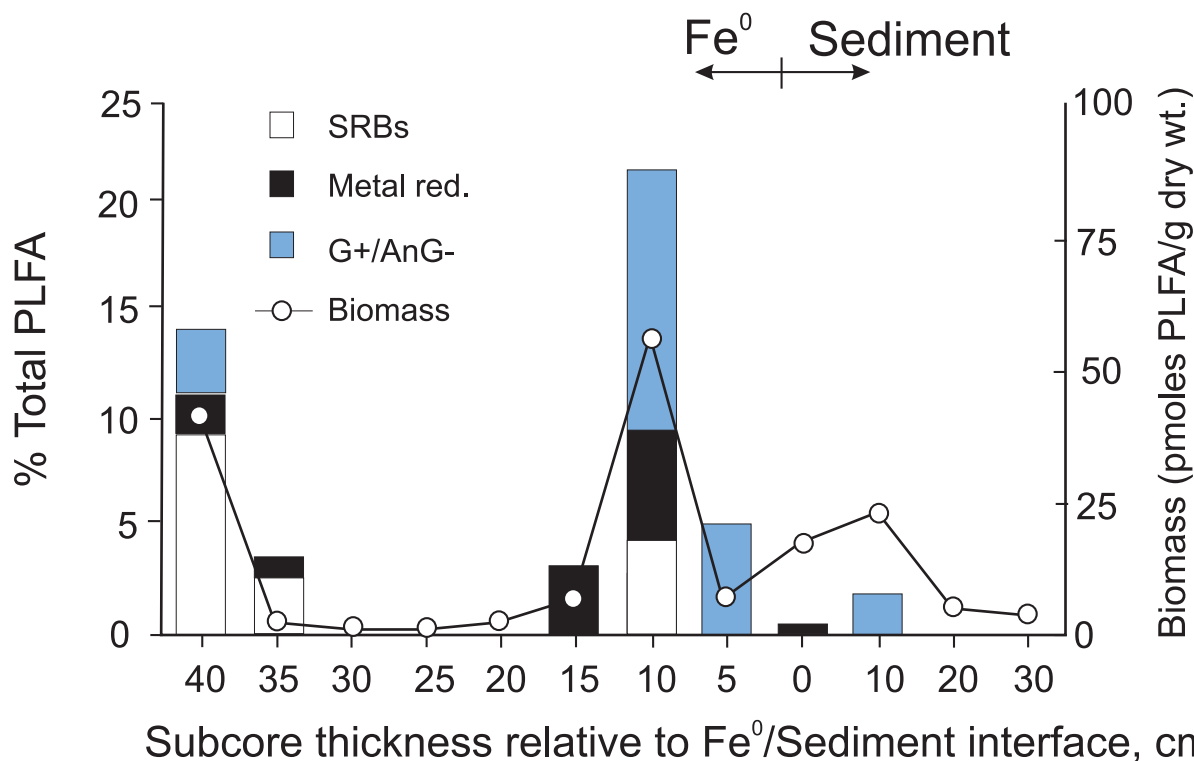


**Figure 13.** Concentration and distribution of PLFA in Fe<sup>0</sup> from Elizabeth City (downgradient iron/aquifer region; core EC060300-6).

### Summary: PRB Long-term Performance

The types of mineral precipitates that form in Fe<sup>0</sup> barriers are consistent with those predicted with geochemical models. The principal factors that determine the amount of mineral precipitation and the spatial distribution of precipitates in reactive iron media are flow rate, groundwater chemistry, and microbial community structure. After four years of operation, the Elizabeth City and DFC reactive barriers have developed consistent patterns of spatially heterogeneous mineral precipitation and microbial activity. The development of precipitation and biomass fronts result from the abrupt geochemical changes that occur at upgradient interface regions coupled with groundwater mass flux. Upgradient regions at both sites investigated in this study have witnessed the greatest accumulation of mineral mass and biomass. Neither of the sites of this study show complete filling of available pore space after four years, suggesting that flow characteristics should not be affected by the accumulation of authigenic components. However, even relatively thin coatings of mineral precipitates that do not affect flow patterns may affect the reactivity of iron particles with respect to the degradation of chlorinated organic compounds by diminishing electron flow capacity. At Elizabeth City, chromium concentrations have been reduced to less than 0.01 mg/L and detectable concentrations of chromium have not been observed in any of the downgradient compliance wells since November, 1996. Similarly, concentrations of chlorinated organic compounds (TCE, cis-DCE, VC) at Elizabeth City are below regulatory target levels in downgradient compliance wells. At the DFC, treatment of chlorinated compounds with Fe<sup>0</sup> has been equally successful in gates 1 and 3. In gate 2, detection of 1,1-DCE at downgradient sampling points has been linked to impacts of the funnel-and-gate system on groundwater flow and

bypass of contaminants underneath the reactive zone or residual contamination in downgradient sediments (McMahon et al., 1999). Contaminant breakthrough, particularly of 1,1-DCE is likely related, either directly or indirectly, to anomalous buildup of authigenic precipitates and biomass on the iron surfaces which could cause a loss of effective reactivity, and therefore decreased efficiency of contaminant degradation processes in the reactive media. Residual contamination downgradient of gate 2 is also a likely source of contaminants (FHWA, 1999). In addition to mineral/biomass accumulation in gate 2, potential indicators of decreased performance are increased Eh values, decreased dissolved hydrogen values, increases in relative specific conductance values and concentrations of certain solutes, such as sulfate and magnesium.

### Acknowledgments

We thank F. Beck, P. Clark, M. McNeil, C. Paul, F. Kahn, K. Jones, and J. Cloud for invaluable field and laboratory assistance. We also gratefully acknowledge the support provided by ManTech Environmental Research Services Corp. J. P. Messier (USCG) is thanked for providing site assistance at the USCG-SC and C. Eriksson (FHWA) and J. Jordan (FHWA) are thanked for site assistance at the DFC.

### Notice

The U. S. Environmental Protection Agency through its Office of Research and Development funded the research described here. This research brief has been subjected to the Agency's peer and administrative review and approved for publication as an EPA document. Mention of trade names or commercial products does not constitute endorsement or recommendation for use.

## References

- Battelle. *Recommendations for Modeling the Geochemical and Hydraulic Performance of a Permeable Reactive Barrier*, Prepared for Naval Facilities Engineering Service Center: Port Hueneme, CA, 2000.
- Beck, F., Clark, P., and Puls, R. *Ground Water Mon. Rem.* 2000, 20, 55-59.
- Benning, L. G., Wilkin, R. T., Barnes, H. L. *Chem. Geol.* 2000, 167, 25-51.
- Bethke, C. M. The Geochemist's Workbench, version 3.0, A users guide to Rxn, Act2, Tact, React, and Gtplot. University of Illinois, Urbana 1998, 184 pp.
- Blowes, D.W., Gillham, R.W., Ptacek, C.J., Puls, R.W., Bennett, T.A., O'Hannesin, S.F., Bain, J.G., Hanton-Fong, C.J., Bain, J.G. EPA/600/R-99/095a 1999, 111 pp.
- Blowes, D.W., Puls, R.W., Gillham, R.W., Ptacek, C.J., Bennett, T.A., Bain, J.G., Hanton-Fong, C.J., Paul, C.J. EPA/600/R-99/095b 1999, 207 pp.
- Blowes, D. W., Mayer, K. U. EPA/600/R-99/095c 1999, 38 pp.
- Bonin, P. M. L., Odziemkowski, E. J., Reardon, E. J., Gillham, R. W. *J. Sol. Chem.* 2000, 29, 1061-1074.
- Bourrié, G., Trolard, F., Génin, J., Jaffrezic, A., Maître, V., Abdelmoula, M. *Geochim. Cosmochim. Acta.* 1999, 63, 3417-3427.
- Butler, E. C., Hayes, K. F. *Environ. Sci. Technol.* 2000, 34, 422-429.
- Cantrell, K. J., Kaplan, D. I., Wietsma, T. W. *J. Haz. Mat.* 1995, 42, 201-212.
- Chapelle, F. H., Vroblesky, D. A., Woodward, J. C., Lovely, D. R. *Environ. Sci. Technol.* 1997, 31, 2873-2877.
- Cord-Ruwish, R. *Environmental Microbe-Metal Interactions*, ASM Press: Washington, D.C., 2000, 159-173.
- Dowling, N.J.E., Widdel, F., White, D. C. *J. Gen. Microbiol.* 1986, 132, 1815-1825.
- Edlund, A., Nicols, P. D., Roffey, R., White, D. C. *J. Lipid Res.* 1985, 26, 982-988.
- FHWA. IM#1 Performance Evaluation Report. 1999.
- Gavaskar, A. R., Gupta, N., Sass, B. M., Jansoy, R. J., O'Sullivan, D. *Permeable Barriers for Groundwater Remediation Design, Construction, and Monitoring*, Battelle Press: Columbus, OH, 1998.
- Génin, J., Refait, P., Bourrié, G., Abdelmoula, M., and Trolard, F. *Appl. Geochem.* 2001, 16, 559-570.
- Guckert, J.B., Antworth, C.P., Nicols, P.D., White, D.C. *FEMS Microbiol. Ecol.* 1985, 31, 147-158.
- Herbert, R. B., Benner, S. G., Blowes, D. W. *Appl. Geochem.* 2000, 15, 1331-1343.
- Hernandez, G., Kucera, V., Thierry, D., Pedersen, A., Hermansson, M. *Corrosion* 1994, 50, 603-608
- Hsü, K. J. Chemistry of dolomite formation. In Carbonate rocks: Origin, Occurrence, and Classification (G. Chilingar, H. Bissel, and R. Fairbridge, eds.), 1967, Elsevier, Amsterdam, pp. 169-191.
- Lee, W., Andowski, Z.L., Nielsen, P.H., Hamilton, W.A. *Biofouling* 1995, 8, 165-194.
- Liang, L., Korte, N., Gu, B., Puls, R., Reeter, C. *Adv. Environ. Res.* 2000, 4, 273-286.
- Mackenzie, P. D., Horney, D. P., Sivavec, T. M. *J. Haz. Mat.* 1999, 68, 1-17.
- Mayer, K. U., Blowes, D. W., Frind, E. O. *Water Resour. Res.* 2001, 37, 3091-3103.
- McGill, I. R., McEnaney, B., Smith, D.C. *Nature* 1976, 259, 200-201.
- McMahon, P. B., Dennehy, K. F., Sandstrom, M. W. *Ground Water* 1999, 37, 396-404.
- Morales, J., Esparza, P., Gonzalez, S., Salvarezza, R., Arevalo, M.P. *Corros. Sci.* 1993, 34, 1531-1540.
- Morrison, S. J., Metzler, D. R., Carpenter, C. E. *Environ. Sci. Technol.* 2001, 35, 385-390.
- O'Hannesin, S. F., Gillham, R. W. *Ground Water* 1998, 36, 164-170.
- Parkes, R. J., Dowling, D. C., White, D. C., Herbert, R. A., and Gibson, G. R. *FEMS Microbiol. Ecol.* 1992, 102, 235-250.
- Phillips, D. H., Gu, B., Watson, D. B., Roh, Y., Liang, L., Lee, S. Y. *Environ. Sci. Technol.* 2000, 34, 4169-4176.
- Powell, R. M., Puls, R. W., Hightower, S. K., Sabatini, D. A. *Environ. Sci. Technol.* 1995, 29, 1913-1922.
- Pratt, A. R., Blowes, D. W., Ptacek, C. J. *Environ. Sci. Technol.* 1997, 31, 2492-2498.
- Puls, R. W., Powell, R. M. *Ground Water Mon. Rev.* 1992, Summer, 130-141.
- Puls, R. W., Paul, C. J., Powell, R. M. *Appl. Geochem.* 1999, 14, 989-1000.
- Reardon, E. J. *Environ. Sci. Technol.* 1995, 29, 2936-2945.
- Scherer, M. M., Richter, S., Valentine, R. L., Alvarez, P. J. J. *Crit. Rev. Environ. Sci. Technol.* 2000, 30, 363-411.
- Schwertmann, U., Fechter, H. *Clay Min.* 1994, 29, 87-92.
- Schwertmann, U., Taylor, R. M. Minerals in Soil Environments, eds. J.B. Dixon and S. B. Weed, Soil Science Society of America Book Series, No. 1, 1989, Ch. 8, pp. 379-438.
- Trudinger, P. A., Chambers, L. A., Smith, J. W. *Can. J. Earth Sci.* 1985, 22, 1910-1918.
- Vogan, J.L., Focht, R.M., Clark, D. K., Graham, S. L. *J. Haz. Mat.* 1999, 68, 97-108.
- Von Wolzogen Kuehr, C.A.H, van der Vlugt, I.S. *Water* 1934, 18, 147-165.
- White, D.C., Bobbie, R.J., Nikels, J. S., Fazio, S. D., Davis, W. M. *Botanica Mar.* 1980, 23, 239-250.
- Zhabina, N.N. and Volkov, I.I. Environmental Biogeochemistry and Geomicrobiology, ed. W. Krumbein, Ann Arbor Science Publishers, 1978, pp. 735-746.



United States  
Environmental Protection  
Agency

National Risk Management  
Research Laboratory  
Cincinnati, OH 45268

Official Business  
Penalty for Private Use  
\$300

EPA/600/S-02/001  
March 2002

Please make all necessary changes on the below label,  
detach or copy, and return to the address in the upper  
left-hand corner.

If you do not wish to receive these reports CHECK HERE ;  
detach, or copy this cover, and return to the address in the  
upper left-hand corner.

PRESORTED STANDARD  
POSTAGE & FEES PAID  
EPA  
PERMIT No. G-35